JPP Journal of Pharmacy and Pharmacology

JPP 2003, 55: 617–630

Received October 15, 2002
Accepted February 4, 2003
DOI 10.1211/0022357021125
ISSN 0022-3573

Kinetics of metabolism and degradation of mometasone furoate in rat biological fluids and tissues

X. W. Teng, D. J. Cutler and N. M. Davies

Abstract

Mometasone furoate (MF) is a potent glucocorticoid developed for the treatment of glucocorticoid-responsive inflammatory disorders. The in-vitro and ex-vivo kinetics of the degradation and metabolism of MF were studied in selected biological fluids of rat and subcellular fractions of different rat tissues. In-vitro, MF was found to degrade slowly into four products in serum and urine, and metabolized rapidly and extensively in rat liver, minimally in extrahepatic tissues, including intestine, stomach, lung and kidney. Further investigation found that the microsomal fraction was the major intracellular site of MF 6β-hydroxylation in rat liver. Using chemical inhibitors, CYP3A was found to be the major enzyme involved in the in-vitro MF 6β-hydroxylation in rat liver microsomes. Enzyme kinetic studies in rat liver microsomes showed that the overall metabolic process of MF followed biphasic Michaelis-Menten kinetics, while 6β-hydroxylation obeyed monophasic Michaelis-Menten kinetics. The kinetic parameters derived from the kinetic models along with the enzyme inhibition studies suggest that MF is mainly metabolized via 6β-hydroxylation mediated by CYP3A primarily, and also biotransformed via other pathway(s) catalysed by other enzymes in rat liver in-vitro.

Introduction

Mometasone furoate (MF) is a potent glucocorticoid with an improved ratio between local to systemic effects. It has been marketed as a dermatological formulation (Elocon), an aqueous intranasal spray (Nasonex), and a dry-powder inhaler (Asmanex Twisthaler) for the treatment of glucocorticoid-responsible dermatoses (Prakash and Benfield 1998) and airway allergic inflammatory disorders (Onrust and Lamb 1998). After oral (Wang et al 1992), dermatological (Prakash & Benfield 1998), intranasal (Onrust & Lamb 1998) or inhalational (Affrime et al 2000a) administration of MF in humans, its systemic exposure is negligible and the bioavailability is very low ($< 1\%$). Following the administration of MF via a metered-dose inhaler, the deposition pattern of MF is consistent with the 10–20% pulmonary and 80% oropharynx deposition demonstrated with other corticosteroids delivered in the same manner (Pickering et al 2000). It has been postulated that the extremely low bioavailability of inhaled MF is owing to extensive metabolism of the drug in the liver following its absorption through respiratory and gastrointestinal tracts (Affrime et al 2000b). However, to date, there is limited information available on the metabolism of MF. An abstract reported that MF was metabolized extensively in the liver, to some extent in the intestine, but not in the lungs of different species in-vitro, including rat, mouse, dog and human, with 6β-hydroxy-MF suggested to be the major metabolite in rat, while other moderately polar metabolites are also present in mouse, dog and human (Zbaida et al 1997). It has not been known if metabolites of MF are active or inactive. The most recent review on MF (Sharpe & Jarvis 2001) quoted both published and unpublished results, and stated that MF is metabolized extensively into polar compounds by cytochrome P450 (P450) 3A4 in the liver, but no evidence of a single major metabolite and no metabolites have been unequivocally identified. Thus, these previous statements on metabolite(s) of this drug remain unclear.

The purpose of the present studies was to qualitatively and quantitatively investigate the in-vitro and ex-vivo kinetics of degradation and metabolism of MF in a rat

Department of Pharmaceutical Sciences, College of Pharmacy and Center for Integrated Biotechnology, Washington State University, Pullman, Washington, USA

X. W. Teng, N. M. Davies

Faculty of Pharmacy, University of Sydney, Sydney, New South Wales, Australia

D. J. Cutler

Correspondence: N. M. Davies, Washington State University, College of Pharmacy, Department of Pharmaceutical Sciences, PO Box 646534, Pullman, WA 99164-6534, USA. E-mail: ndavies@wsu.edu

Acknowledgements: The authors would like to thank Schering-Plough Australia Pty Ltd (Baulkham Hills, NSW, Australia) for a donation of mometasone furoate and the assistance of Mr Bruce Tattam and Dr A. Cheung in chemical analysis.

model. The specific objectives of the present studies were: (i) to determine the major site(s) of MF metabolism in rats; (ii) to investigate the contribution of microsomal enzymes towards the biotransformation of MF in rats; (iii) to analyse the enzyme kinetics of MF in rat liver microsomes and develop kinetic models describing the metabolism of MF in rats; and (iv) to isolate and purify the major degradation and metabolic products from suitable in-vitro systems in rats for its further pharmacological study.

Materials and Methods

Materials

Authentic MF was a gift from Schering-Plough Pty Ltd (Baulkham hills, NSW, Australia). Testosterone 17-acetate, halothane, Krebs-Henseleit buffer, total protein reagent, protein standard solution, monosodium glucose-6-phosphate, β-nicotinamide adenine dinucleotide phosphate (β-NADP) sodium salt hydrate, glucose-6-phosphate dehydrogenase, HEPES (*N*-[2-hydroxyethyl] piperazine-*N*′-[2-ethane sulfonic acid]), 1-aminobenzotriazole, furafylline, coumarin, sulfaphenazole, diazepam, quinidine, diethyldithiocarbamate, 4-methylpyrazole, ketoconazole and troleandomycin were purchased from Sigma Chemical (St Louis, MO, USA). Medical carbogen gas (containing 5% carbon dioxide and 95% oxygen) and high purity nitrogen gas were purchased from BOC Gases (Chatswood, NSW, Australia). Carbon monoxide was obtained from Matheson Tri-Gas, Inc. (Newark, CA, USA). All other chemicals and solvents were of analytical or HPLC grade as appropriate.

Animals and collection of biological fluids and tissues

Adult male Sprague-Dawley rats, 200–250 g, were supplied by the Laboratory Animal Services Center at the University of Sydney. The rats were allowed free access to standard laboratory chow (Purina Rat Chow; Ralston, Sydney, NSW, Australia) and tap water, and were maintained in a restricted access room with controlled temperature (21 ± 1 °C), humidity and a 12-h light/dark cycle. The experimental animal protocols were approved by the Animal Ethics Committee of the University of Sydney.

Rat urine was collected from individual rats housed in metabolic cages (Technoplast, Rochester, NY, USA) for 0–24 h. After the rats were anaesthetized with 5% (v/v) halothane, the blood was collected via terminal cardiac puncture. Subsequently, a vertical midline abdominal incision was made, and the tissues required were rapidly excised, examined and immediately placed in ice-cold 10 mM Tris-buffered saline (pH 7.5). Blood was allowed to clot and then centrifuged to yield serum, which was stored at −20 °C. The pH of the pooled rat serum was 7.36, measured before the kinetic study.

Preparation of tissue subcellular fractions

Rat tissues were homogenized using a Polytron PTA 1035 homogenizer (Kinematica GmbH, CH-6010, Kriens/Luzerne, Switzerland) and the 1000 *g* supernatant (S-1), 9000 *g* supernatant (S-9), cytosolic and microsomal fractions of individual tissue were prepared by differential centrifugation (Ekins et al 1999). Pooled nuclear, mitochondrial, cytosolic and microsomal fractions of rat liver tissue ($n = 6$) were also prepared by differential centrifugation (Pedersen et al 1978). All the homogenization and fractionation processes were conducted in a cold room at −4 °C. The subcellular fractions of tissues were stored at −80 °C before use. Total protein contents of the fractions of tissue homogenates were determined spectrophotometrically at 540 nm (Doumas et al 1981). Bovine serum albumin was used as the reference standard. The P450 content was determined as described previously (Ocuma & Sato 1964).

Instrumentation and analytical methods

HPLC analysis of MF and its degradation and metabolic products was performed as previously described (Teng et al 2001). The Shimadzu Class-LC10 HPLC (Kyoto, Japan) system consisted of an LC-10AT pump, a SIL-10AXL autoinjector, an FRC-10A fraction collector, an SPD-M10A photodiode-array UV/vis spectrophotometric detector and a CBM-10A communication bus module. Data collection and integration were accomplished using Shimadzu Class-LC10 computer software version 1.64 (Kyoto, Japan). The analytical column used was a Beckman ultrasphere octyl column (150 mm, 2.0 mm i.d., 5 μm particle size; Beckman Instruments, Fullerton, CA, USA) equipped with a pre-column (7.5 mm, 2.0 mm i.d.) of the same packing material. The mobile phase consisted of methanol and water (59:41, v/v), filtered and degassed using a Millipore filtration system through a 0.45-μm HNWP nylon filter (Bedford, MA, USA) under reduced pressure before use. Separation was carried out isocratically at room temperature (22 ± 1 °C) and with flow rate of 0.28 mL min^{-1}, with UV detection at 248 nm and spectral scanning from 200 to 400 nm. The injection volume was 10 μL.

Kinetics of MF in rat serum and urine

MF ($C_0 = 19$ μM, added as a methanolic stock solution of 2.0 mg mL^{-1} at a volume of 0.5% in the final incubation mixtures) was incubated in rat urine and in rat serum at 37.0 ± 0.1 °C in a thermostatically controlled shaking water bath as described previously (Teng et al 2001).

Kinetics of MF in rat tissue S-9 fractions

Studies of metabolic kinetics of MF in S-9 fractions of tissue homogenates were conducted in the presence of cofactors that included 10 mM $MgCl_2$ and an NADPH-generating system (7.5 mM glucose 6-phosphate, 0.3 mM β-NADP and 0.42 units mL^{-1} glucose-6-phosphate

dehydrogenase), in 100 mM phosphate buffer containing 1 mM EDTA (pH 7.4) under carbogen gas at 37.0 ± 0.1 °C in a shaking (75 rev min^{-1}) water bath. Typically, the S-9 fraction (protein content 4 mg mL^{-1}, unless otherwise indicated) and the parent drug ($C_0 = 19\ \mu M$, added as a methanolic stock solution of 2.0 mg mL^{-1} at a volume of 0.5% in the final incubation mixtures) were pre-incubated in the incubation buffer for 5 min at 37 ± 0.1 °C. The reaction was initiated by adding the cofactors. At predetermined time intervals, samples (0.5 mL each) were withdrawn and the reaction was terminated immediately by adding 4 mL ice-cold dichloromethane. Samples were then extracted and analysed by HPLC (Teng et al 2001). Parallel incubations were performed in the same manner in the absence of MF or the S-9 fraction as controls. Experiments with the tissue S-9 fractions were performed in four replicates.

The metabolic kinetics of MF in pooled rat liver tissue S-9 fractions was investigated with respect to protein concentration (range 1–8 mg mL^{-1}) and substrate concentration (range 1–100 μM).

Studies of degradation kinetics of MF ($C_0 = 19\ \mu M$, added as a methanolic stock solution of 2.0 mg mL^{-1} at a volume of 0.5% in the final incubation mixtures) in each S-9 fraction of the rat tissues were carried out without cofactors. The reaction was initiated by adding the stock MF in the reaction media and then handled using the same method.

Kinetics of MF in rat liver microsomal, cytosolic, mitochondrial and nuclear fractions

Initially, the microsomal incubation conditions were investigated with respect to microsomal protein concentration (0.1–5 mg mL^{-1}), incubation time (up to 60 min), substrate concentration (0.2–100 μM), and oxygenation using pooled rat liver microsomes. The optimized microsomal incubation mixture was composed of liver microsomes (0.2 mg protein mL^{-1}), 2.5 μM MF and an NADPH-generating system (6 mM $MgCl_2$, 0.5 mM β-NADP, 10 mM glucose 6-phosphate and 1.0 units mL^{-1} glucose-6-phosphate dehydrogenase) in 100 mM phosphate buffer containing 1 mM EDTA (pH 7.4). The reaction was carried out in open test tubes without extra oxygenation for 8 min in a shaking (150 rev min^{-1}) water bath. After the microsomal fraction and the parent drug (added as a methanolic stock solution at a volume of 1% in the final incubation mixtures) were pre-warmed in the incubation buffer for 5 min at 37 ± 0.1 °C, the reaction was initiated by the addition of the NADPH-generating system, and terminated by addition of 4 mL ice-cold dichloromethane. Similar incubations with the use of denatured microsomes (heating at 70–80 °C for 30 min) or without the addition of microsomes or substrate were conducted in the same manner as controls. In addition, incubation in the absence of the NADPH-generating system was performed for the confirmation of P450-dependent enzymatic biotransformation. Typically, all the incubations of MF ($C_0 = 4\ \mu M$) with microsomal, cytosolic, mitochondrial and nuclear fractions (protein content 4 mg mL^{-1}) were performed following the same procedure. Incubations for each individual condition with these subcellular fractions of rat liver tissue were conducted in duplicate.

Kinetics in everted rat small intestine tissue

A modified version of the method of Esposito & Csaky (1974) was employed in these studies. After anaesthetization of the rat with halothane, an abdominal incision was made and the whole small intestine was isolated, excised and examined. After a section (~10 cm) of intestine at the end of the ileocecal junction was taken for tissue sample of zero time, the intestine was immediately flushed with ice-cold Krebs-Henseleit bicarbonate buffer containing 2 g L^{-1} glucose (pH 7.4; K-H buffer), and then everted on a glass rod with one end tied with surgical thread. After the sac was filled with warmed drug-free K-H buffer (37 °C), the other end was tied and the middle part of the intestine was tied every 20–25 cm to give four isolated sections. This everted intestine was immediately placed in a freshly prepared, warmed (37 °C) and jacketed beaker containing 25 mL of 19 μM MF (10 μg mL^{-1}, added as a methanolic stock solution of 2.0 mg mL^{-1} at a volume of 0.5% in the final incubation mixtures) in K-H buffer, and incubated at 37 ± 0.1 °C with continual carbogenation with carbogen in a shaking water bath (75 rev min^{-1}).

The zero-time buffer sample (the K-H buffer with drug) was withdrawn before the tissue was placed in the K-H buffer and the drug-free K-H buffer was used as the zero-time buffer sample in the sac. At 0.5, 1.5, 3 and 5 h, 3 mL of buffer in the bulk incubation medium and a section of the intestine (about 2 g) with the buffer in its lumen were sampled. After the buffer in the lumen was transferred into a beaker, the tissue segment was weighed and then immediately added to ice-cold K-H buffer of equal weight. Subsequently, the tissue was minced, homogenized, extracted and analysed by HPLC.

Buffer samples (0.5 mL) from both the bulk incubation medium and the intestinal lumen were also collected for analysis of MF and its degradation and metabolic products as described for samples of tissue subcellular fractions. The experiment was performed in triplicate.

Inhibition studies

A number of potential inhibitors and/or substrates of CYP isoenzymes were tested at various concentrations in pooled rat liver microsomes (protein content 0.2 mg mL^{-1}) with varying concentrations of MF (added as a stock methanolic solution at a volume of 1% in the final incubation mixtures). Incubation mixtures containing mechanism inhibitors, furafylline, diethyldithiocarbamate, troleandomycin, or 1-aminobenzotriazole, were pre-incubated in pooled rat liver microsomes in the presence of the NADPH-generating system (6 mM $MgCl_2$, 0.5 mM β-NADP, 10 mM glucose-6-phosphate and 1.0 units mL^{-1} glucose-6-phosphate dehydrogenase) at 37 ± 1 °C for 15 min before the addition of MF. For non-mechanism-based inhibitors, the incubation mixtures

contained MF and inhibitors together with rat liver microsomes without pre-incubation of inhibitors, and the reactions were initiated by the addition of the NADPH-generating system and carried out as for rat liver microsomes. Potential inhibitors were dissolved in a mixture of methanol and phosphate buffer, except for ketoconazole, which was dissolved in acetone, and added at a volume of 1% in the final incubation mixtures. Parallel control incubations were conducted with 1% of the corresponding solvent with no inhibitor present. Each potential inhibitor was also incubated with microsomes under the NADPH-generating system to examine if they caused any chromatographic interference in the measurement of 6β-hydroxy-MF.

Sample extraction and analysis

For tissue and sub-cellular fractions, on terminating the reaction with 4.0 mL ice-cold dichloromethane, 0.5 mL of internal standard (10 μg mL^{-1} of ethanolic testosterone 17-acetate) was added to the sample (0.5 mL). The mixture was extracted for 2 min on a vibrating mixer, followed by centrifugation at 1328 g (20 °C) for 10 min. The organic layer was then collected, evaporated to dryness under nitrogen at 35 °C, stored at −20 °C and reconstituted in mobile phase before HPLC analysis.

To each sample (0.5 g) of tissue homogenate was added 0.5 mL of internal standard (10 μg mL^{-1} ethanolic testosterone 17-acetate). The mixture was extracted twice with 4 mL dichloromethane by vigorous shaking for 2 min on a vibrating mixer, followed by centrifugation at 2602 g (20 °C) for 10 min. The dichloromethane phase was collected, evaporated, stored at −20 °C and reconstituted in mobile phase before HPLC analysis.

Data analysis

Data are expressed as the mean ± s.d. of replicate determinations ($n \geqslant 5$). Statistical analyses were performed using Microsoft Excel (version 97) or SPSS (Spss Inc., IL, USA). Significance of differences in means of paired samples was assessed using a paired-sample t-test. Analysis of variance of two or more groups of data was performed using analysis of variance and Tukey's post-hoc analysis. All values of P were based on two-tailed tests and P values of less than 0.05 were considered statistically significant.

The observed rate constants (k_{obs}) of parent drug disappearance were estimated from the initial slope of the log-linear phase of declining concentration versus time plots. The initial half-lives were calculated using the following equation: $t_{1/2} = 0.693/k_{obs}$. The rate constant of each metabolic reaction was estimated according to the corresponding model developed, based on the experimental data, to limit underestimation of the parameters due to possible sequential transformation. The rate constant of parent drug disappearance was correlated to the sum of those of its direct transformation reactions.

Substrate concentrations ranging from 0.2 to 100 μM were employed for MF in view of its unknown in-vitro metabolic kinetics in rat liver microsomes. Kinetic analysis of the parent drug disappearance and product formation data was undertaken by the least-square regression program using SCIENTIST version 2.0 (Micromath Scientific Software, Salt Lake City, UT, USA). Apparent enzyme kinetics was determined by fitting reaction velocity (v) versus substrate concentration, [MF]. Initially, the data were examined on Eadie-Hofstee, Lineweaver-Burk and Hanes plots to assess the linearity of enzyme kinetics. The kinetic data were then fitted to expressions containing one or more Michaelis-Menten terms. The correlation, randomness of the residuals, the standard deviation of the parameter estimates (< 10%) and the model selection were used as indicators of goodness-of-fit of the model to the experimental data.

The nature of inhibition of the chemical inhibitors for P450 was initially assessed by plots from transformed data from the kinetic studies, including Dixon plot, Lineweaver-Burk plot, Eadie-Hofstee plot, and Cornish-Bowden plot. For competitive enzyme inhibitors, the apparent inhibitory constant (K_i) was given by the intersection point of linear regression lines in the Dixon plot, where data sets of 1/v were plotted against the initial concentration of the inhibitor, [I]. Results were subsequently subjected to Equation 1 (Ito et al 1998) by least-square regression using SCIENTIST.

$$\nu = \frac{V_{max} \cdot [MF]}{K_m \cdot \left(1 + \frac{[I]}{K_i}\right) + [MF]} \quad (1)$$

where K_m represents the Michaelis constant of the enzymatic reaction (cf. Equation 5), [MF] is the initial drug concentration, and V_{max} indicates the maximum velocity of the reaction.

Kinetic parameters for mechanism-based enzyme inactivation were obtained as described by Ito et al (1998). The logarithm of the remaining enzymatic activity (formation rate of 6β-hydroxy-MF) was plotted against the pre-incubation time in the presence of the inhibitor at various concentrations. The apparent inactivation rate constant ($k_{i,obs}$) was determined from the slope of the initial linear phase at each inhibitor concentration. The apparent $k_{i,obs}$ values were compared with those of control incubations containing the solvent for each inhibitor as appropriate. The values of $k_{i,obs}$ were plotted against the inhibitor concentrations and the parameters ($k_{i,max}$ and K_i') were estimated from Equation 2 by a non-linear least square method using SCIENTIST.

$$k_{i,obs} = \frac{k_{i,max} \cdot [I]}{K_i' + [I]} \quad (2)$$

where $k_{i,obs}$ is the apparent inactivation rate constant of the enzyme at initial inhibitor concentration [I], $k_{i,max}$ represents the maximum inactivation rate constant, and K_i' represents the apparent dissociation constant between the enzyme and the inhibitor, respectively (Ito et al 1998).

The IC50 (the concentration inhibiting 50% of enzyme activity) was determined by linear regression (percentage of control) against the logarithmic inhibitor concentration.

Results

Degradation in rat serum

MF ($C_0 = 19\ \mu M$) degraded in rat serum (pH 7.36) with a half-life of 8.0 ± 0.1 h ($n = 4$). Four products, namely A, B, C and D (Figure 1), were formed in rank order, and are the same as observed previously in human plasma and in simulated lung fluid (Teng et al 2001; products A, B, C and D reported here correspond to products D1, D3, D2 and D4 reported in Teng et al 2001). They were identified as: A: 21-chloro-17α-hydroxy-16α-methyl-9β,11β-oxidopregna-1,4-diene-3,20-dione 17-(2-furoate); B: 9α,21β-dichloro-11β,21α-dihydroxy-16α-methylpregna-1,4,17, 20-tetraen-3-one 21-(2-furoate); C: 21β-chloro-21 α-hydroxy-16α-methyl-9β,11β-oxidopregna-1,4,17,20-tetraen-3-one 21-(2-furoate); and D: 21-chloro-17α-hydroxy-16α-methyl-9β,11β-oxidopregna-1,4-diene-3,20-dione (Teng 2002).

Degradation in rat urine

MF ($C_0 = 19\ \mu M$) degraded in rat urine (pH 7.83) with a half-life of 11.1 ± 0.3 h ($n = 4$). The degradation profile of MF in rat urine was qualitatively similar to that in rat serum.

Metabolism of MF in S-9 fractions of rat tissues

MF ($C_0 = 19\ \mu M$) decomposed quickly with a half-life of 23.3 ± 10.7 min ($n = 6$) and rapid formation of 6β-hydroxy-MF in the rat liver tissue S-9 fractions of protein content 4 mg mL^{-1}. The formation of 6β-hydroxy-MF was not observed in control samples in which the parent drug or the S-9 fractions were absent. In rat liver tissue S-9 fraction, the apparent rate of MF 6β-hydroxylation in the presence of cofactors was over 1000-times greater than that in the absence of cofactors, indicating that this reaction was largely catalysed by enzymes dependent on cofactors.

The apparent rate of MF ($C_0 = 19\ \mu M$) disappearance and formation of 6β-hydroxy-MF increased with an increase in total protein concentration of rat liver tissue S-9 fractions from 1 to 8 mg mL^{-1}. On the other hand, the apparent rates of MF disappearance and 6β-hydroxy-MF formation were both enhanced with an increase in the initial concentration of MF from 1 to 50 μM, but there was no further increase at 100 μM when the total protein of rat liver tissue S-9 fraction was kept constant at 4 mg mL^{-1}.

In addition, the relative activities of the S-9 fractions of the tested extrahepatic tissues catalysing MF 6β-hydroxylation were less than 1% of that of the rat liver tissue. In these S-9 fractions, the apparent rates of MF 6β-hydroxylation were in the order of: intestine $\geqslant$ stomach $>$ spleen $>$ kidney $>$ lung. In the rat lung tissue S-9 fraction, 6β-hydroxy-MF was detectable but not quantifiable in about half of the samples using the HPLC/UV assay.

In the presence of cofactors, the rate of degradation of MF through the formation of products A, B, C and D was much slower than in the corresponding tissue S-9 fractions without cofactors ($P < 0.01$, paired-sample t-test). In fact, only product A (not B, C or D) was detectable during incubation up to 72 h in all S-9 fractions of tissues tested with cofactors.

Metabolism in rat liver subcellular fractions

MF was metabolized rapidly in rat liver microsomes, with 6β-hydroxy-MF as a primary metabolite (Figure 2), under an NADPH-generating system. No significant transformation of MF to 6β-hydroxy-MF was detected in the controls. As in the S-9 fraction of rat liver tissue, none of the other potential metabolites listed by Affrime et al (2000a) were observed except for 6β-hydroxy-MF.

In pooled liver microsomes from six rats, the apparent rate of both parent drug disappearance and 6β-hydroxy-MF appearance increased with an increase in protein concentration over the range of 0.1 to 5 mg mL^{-1} when an initial concentration of MF was kept at 4 μM.

When total protein of rat liver microsomes was kept constant at 0.2 mg mL^{-1}, the apparent rate of parent drug disappearance (Figure 3) increased with an increase in the initial drug concentration from 0.2 to 65 μM. The decline of MF followed first-order degradation kinetics in rat liver microsomes of protein content 0.2 mg mL^{-1}. The rate of 6β-hydroxy-MF formation increased correspondingly with increasing initial drug concentration from 0.2 to 8 μM. However, the formation was saturated at higher concentrations, reaching a plateau. An optimal incubation time of 8 min was selected as a convenient common incubation time for studying the kinetics of MF metabolism in rat liver microsomes of protein content 0.2 mg mL^{-1}.

Little formation of 6β-hydroxy-MF and disappearance of the parent drug were observed following the incubation of MF ($C_0 = 4\ \mu M$) in pooled rat liver cytosolic, mitochondrial and nuclear fractions of protein content 4 mg mL^{-1} at 37 °C (Table 1). The enzyme activities of this cytosolic, mitochondrial and nuclear fractions catalysing 6β-hydroxylation of MF were 0.4, 4.3 and 1.6% of that of pooled rat liver microsomes, respectively.

Transformation in everted rat intestine

Following the incubation of MF ($C_0 = 19\ \mu M$) with everted intestinal tissue in K-H buffer, MF disappeared rapidly from the incubation buffer with considerable formation of 6β-hydroxy-MF as the major metabolite (Figure 4). Meanwhile, most of the parent drug and the metabolite formed were taken up by the intestinal tissue during incubation.

Inhibition of MF 6β-hydroxylation by potential chemical inhibitors

A non-specific CYP inhibitor, 1-aminobenzotriazole (Mathews et al 1985; Carcillo et al 1998), inhibited MF 6β-hydroxylation in pooled rat liver microsomes in a

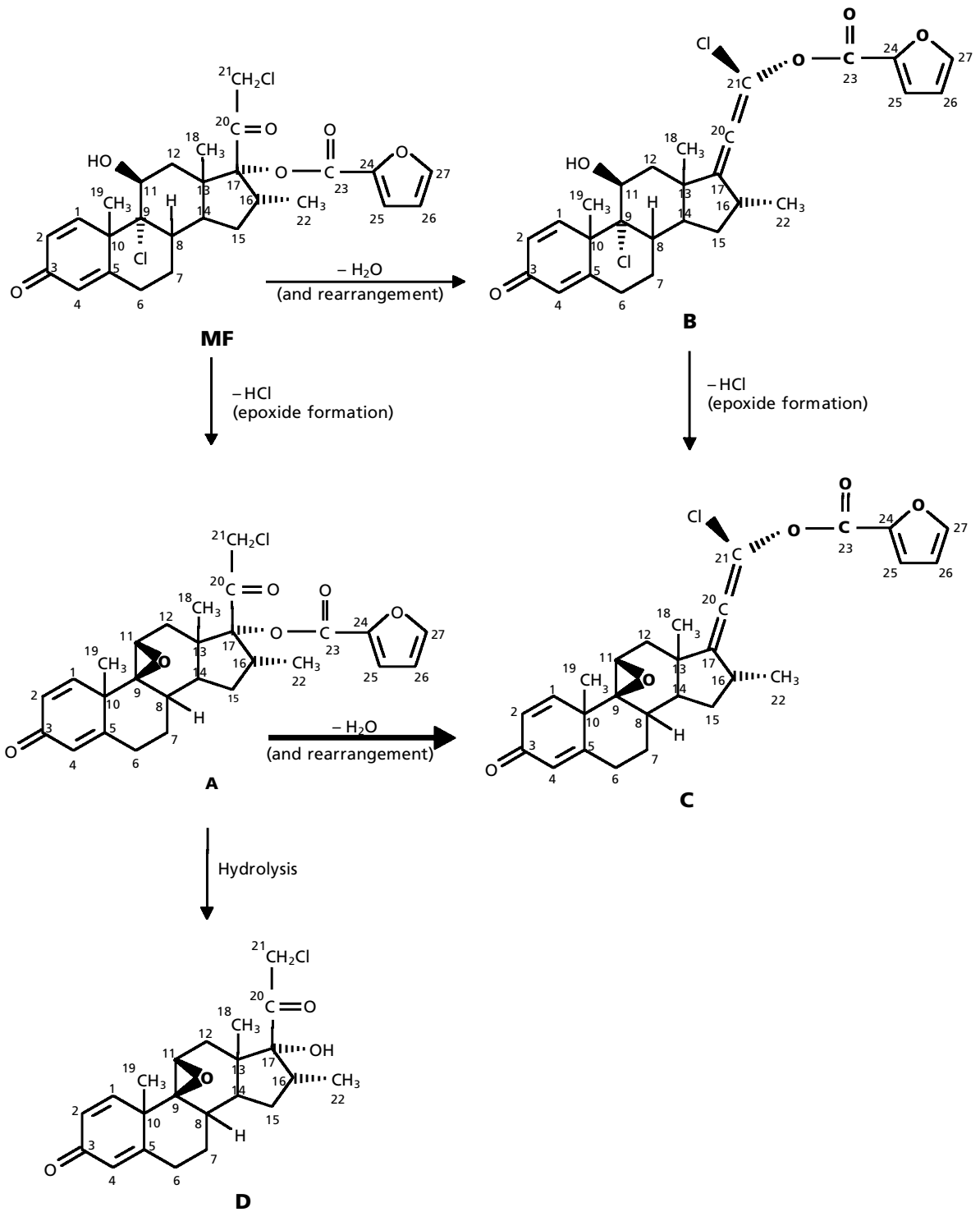

Figure 1 Structures of degradation products of mometasone furoate (MF), with proposed degradation pathways and 21-configuration of products B and C. Thick arrows indicate major pathways.

concentration-dependent manner. Strong inhibition was obtained at low concentrations of ketoconazole, with an apparent K_i of 1.42 μM determined by Equation 1 representing Dixon plots (Figure 5A). Troleandomycin displayed concentration and pre-incubation time-dependent inhibition (Figure 6A) with an apparent K_i' of approximately 177 μM. Diazepam also exhibited considerable competitive inhibition of MF 6β-hydroxylation in rat liver, with an apparent K_i of approximately 88 μM. Moreover, co-incubation with high concentrations

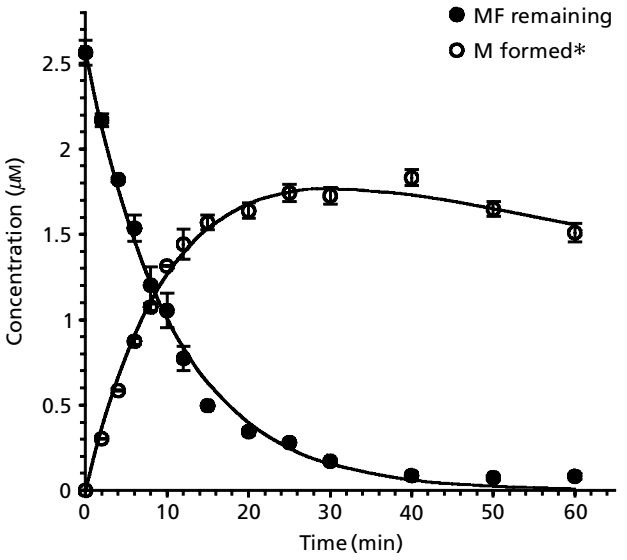

Figure 2 Typical time course for mometasone furoate (MF) ($C_0 = 2.6\,\mu M$) and its metabolite 6β-hydroxy-MF (M) in rat liver microsomes (protein 0.2 mg mL^{-1}) at 37 °C. *The concentration of M formed is expressed relative to the MF concentration, assuming equal HPLC/UV response. Symbols represent mean values and the vertical bars indicate the standard deviation of duplicate determinations. The lines represent simulation using Equations 3 and 4 according to the model for MF metabolism in-vitro (Figure 7).

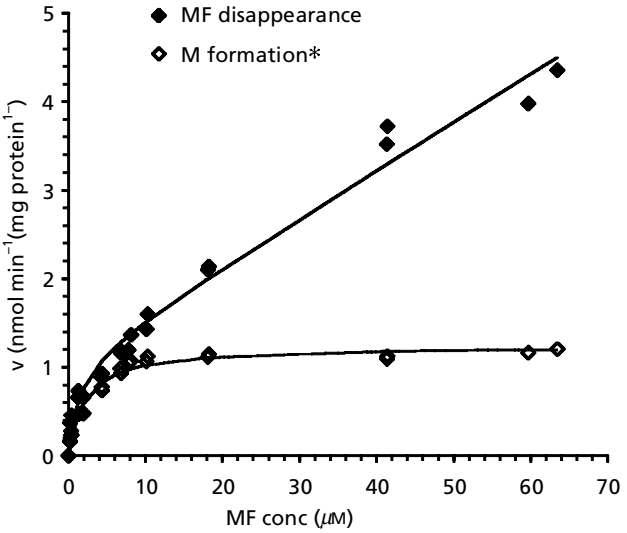

Figure 3 The rates of mometasone furoate (MF) ($C_0 = 0.2 - 65\,\mu M$) disappearance and 6β-hydroxy-MF (M) formation following incubation in pooled rat liver microsomes (protein 0.2 mg mL^{-1}) at 37 °C. Symbols represent experimental data and the lines were fitted by a biphasic Michaelis-Menten model (Equation 7; $V_{max1} = 1.09$ nmol min^{-1} (mg protein)$^{-1}$, $K_{m1} = 1.32\,\mu M$, $CL_2 = 0.054$) and simple Michaelis-Menten equation ($V_{max} = 1.24$, $K_m = 2.15\,\mu M$) for MF and M, respectively. *The concentration of M formed is expressed relative to the MF concentration, assuming equal HPLC/UV response.

(300 and 600 μM) of 4-methylpyrazole caused some decrease in the reaction rate, with an apparent K_i of around 700 μM, provided its inhibition was competitive. Furthermore, diethyldithiocarbamate reduced the reaction rate, with an IC50 of approximately 84 μM. In contrast, furafylline and sulfaphenazole did not exhibit significant inhibition of the reaction at concentrations higher than its effective concentration.

Analysis of kinetics of the in-vitro metabolism of MF in rat liver microsomes

Based on knowledge of the chemical structure, introduction of a hydroxy group at C-6 of the MF molecule would not be expected to cause a significant environmental change to the 1,4-diene-3-one chromophore and the furan-2-carboxyl chromophore. It was evident that 6β-hydroxy-MF exhibited a nearly identical UV spectrum to MF (data not shown). Assuming the HPLC/UV response of 6β-hydroxy-MF was equivalent to that of MF, the high yield of 6β-hydroxy-MF in rat liver tissue S-9 and microsomal fractions indicates that 6β-hydroxylation is the primary metabolic pathway of MF in rat liver in-vitro. The apparent formation of 6β-hydroxy-MF would contribute to approximately 43% of the total loss of the parent drug in rat liver tissue S-9 fraction, estimated from the slopes of the linear regression lines of the apparent rate versus protein concentration. This suggests that MF also undergoes metabolism through other pathways, which can be parallel or subsequent, or both. Except for 6β-hydroxy-MF, under the present experimental conditions, none of the other metabolites postulated by Affrime et al (2000a) were observed in rat liver in-vitro. In addition, the C-17 ester-bond hydoxylated product of MF was not observed in any media tested. The possible reasons of this could be: (i) mometasone was not resolved from other compounds in the HPLC analysis; and (ii) the apparent formation of mometasone was too low. Comparing the chromatograms from Affrime et al (2000a) (in which mometasone, the proposed product of hydrolysis, was eluted after 6β-hydroxy-MF) with those in the present study, mometasone was expected to be eluted after the degradation product D (the hydrolysate of degradation product A) as in parallel relationship of A and MF through the reversed-phase HPLC system used in this study. It was less likely that mometasone fell into the front peaks in the HPLC chromatogram. Therefore, it was likely that the mometasone formed was too low to be detected and/or mometasone was sequentially metabolized to other product(s) that were not resolved by the HPLC method. Thus, a kinetic scheme was proposed for the in-vitro MF metabolism in rat liver (Figure 7). The disappearance of MF, the formation and disappearance of metabolite 6β-hydroxy-MF (M) can be described by differential Equations 3 and 4. As no data were available for N and O, no differential equations for these supposed products were included.

$$[MF]' = -(k_{FM} + k_{FN})[MF] \quad (3)$$

$$[M]' = k_{FM}[MF] - k_{MO}[M] \quad (4)$$

Table 1 Rate of 6β-hydroxy-mometasone furoate (M) formation and the effect of 1-aminobenzotriazole (200 μM) following incubation of mometasone furoate (MF) ($C_0 = 4\,\mu$M, n = 3) in subcellular fractions of rat liver.

Subcellular fraction of rat liver	Rate of M formation (pmol min^{-1} (mg protein)$^{-1}$)	
	Original rate	In the presence of 1-aminobenzotriazole
Microsomes	658.35 ± 28.80	144.78 ± 0.96
Cytosol	2.69 ± 0.41	0.94 ± 0.21
Mitochondria	28.39 ± 2.11	13.15 ± 0.08
Nuclei	10.69 ± 0.41	3.74 ± 0.19

M formed is expressed relative to the concentration of MF, assuming equal HPLC/UV response. Rate of M formation was calculated from the slope of the initial linear phase of M formed.

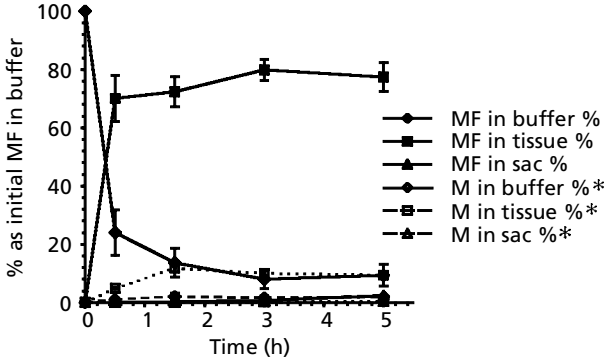

Figure 4 Typical time course for mometasone furoate (MF) and its major metabolite 6β-hydroxy-MF (M) in the K-H buffer incubated with everted rat intestinal tissue. Everted intestinal tissue of rat no. 6 was incubated with MF ($C_0 = 19\,\mu$M = 10 μg mL^{-1}) in 25 mL K-H buffer at 37 °C. *Estimation was made from the peak area ratio of MF and M in samples remaining in the incubation media at each sampling point relative to the initial value of MF, assuming equal HPLC/UV absorbance between MF and M and not taking account of the loss as a result of sampling. Symbols represent the mean values of duplicate experimental data.

Characters in brackets represent the concentrations of parent drug or product at time t, while [X]′ represents the derivates of X with respect to t.

This model was tested by fitting the experimental data of MF obtained from experiments in rat liver microsomes, with curve-fitting performed using SCIENTIST. Good correlation ($r^2 > 0.99$) was obtained between the observed and the predicted values of MF remaining. A typical plot with both experimental and theoretical data is shown in Figure 2.

A better estimation of the 6β-hydroxy-MF formation rate (k_{FM}) was achieved using Equations 3 and 4, compared with the estimation using the apparent 6β-hydroxy-MF concentration in the initial phase. For example, by fitting the observed data to these equations, the relationship between the microsomal protein concentration and the reaction rate constant, for both total loss of MF ($k_{FM} + k_{FN}$) and formation of 6β-hydroxy-MF (k_{FM}), was closer to the real situation. In comparison, the apparent rates of 6β-hydroxylation, obtained from the slopes of initial phase of 6β-hydroxy-MF formation in the concentration–time course, were underestimated by 29 ± 11%. The result was that the apparent contribution of 6β-hydroxylation was averaged at only ~30% of the total loss of MF, given by the slopes of the linear regression lines.

As indicated by the kinetic data in Figure 3, in rat liver microsomes, the relationship between the rate of 6β-hydroxylation and the initial concentration of MF was closely correlated with a monophasic Michaelis-Menten kinetics (Equation 5), with K_m of 1.24 μM and V_{max} of 2.15 nmol min^{-1} (mg protein)$^{-1}$, respectively ($r^2 = 0.9943$, MSC = 3.4; SCIENTIST), whereas the disappearance of the parent drug exhibited atypical Michaelis-Menten kinetics.

$$v = (V_{max}[MF])/(K_m + [MF]) \quad (5)$$

The hyperbolic Michaelis-Menten kinetics for the 6β-hydroxylation was verified by the corresponding Eadie-Hofstee plot, which was nearly linear (Figure 8). This suggests that the reaction involved one enzyme or several enzymes with similar values of K_m in rat liver microsomes. In comparison, the Eadie-Hofstee plot for the loss of the parent drug from the reaction media was clearly concave in nature, which is the feature of allosteric-enzyme kinetics or multiple-enzyme kinetics. The studies using enzyme inhibitors have demonstrated the possibility of involvement of more than one enzyme in MF metabolism. Additionally, as displayed in Figure 3, after 6β-hydroxylation was saturated at high drug concentrations, MF was still metabolized via other routes that were not saturated under the experimental conditions. This provided the information that the catalysing components towards different pathways probably had distinct affinities and capacities. Thus, the multiple-enzyme model (Equation 6) rather than the Hill equation would be more appropriate for describing these kinetic processes.

$$v = \frac{V_{max1} \cdot [MF]}{K_{m1} + [MF]} + \frac{V_{max2} \cdot [MF]}{K_{m2} + [MF]} + \ldots \quad (6)$$

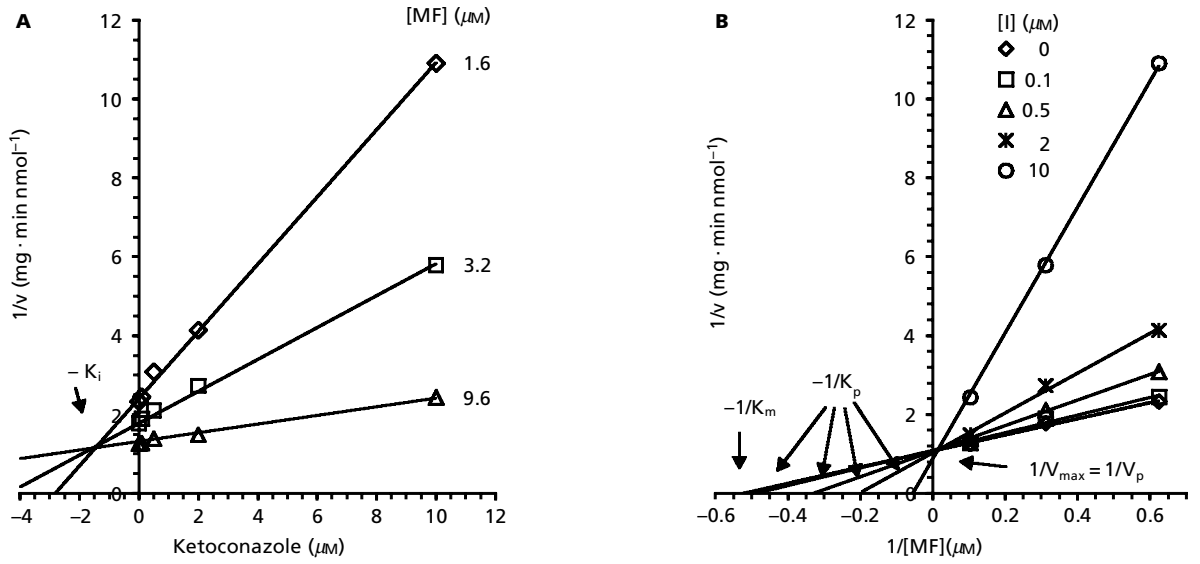

Figure 5 Inhibitory effect of mometasone furoate (MF) 6β-hydroxylation by ketoconazole illustrated by (A) Dixon and (B) Lineweaver-Burk plots. MF (1.6, 3.2 and 9.6 μM) was incubated for 8 min at 37 °C in pooled rat liver microsomes (protein 0.2 mg mL^{-1}) in the presence of 0.1, 0.5, 2 or 10 μM ketoconazole. Symbols representing parameters: K_i, inhibition constant; K_m, Michaelis constant; K_p, Michaelis constant in the presence of enzyme inhibitor; V_p, maximum velocity in the presence of enzyme inhibitor.

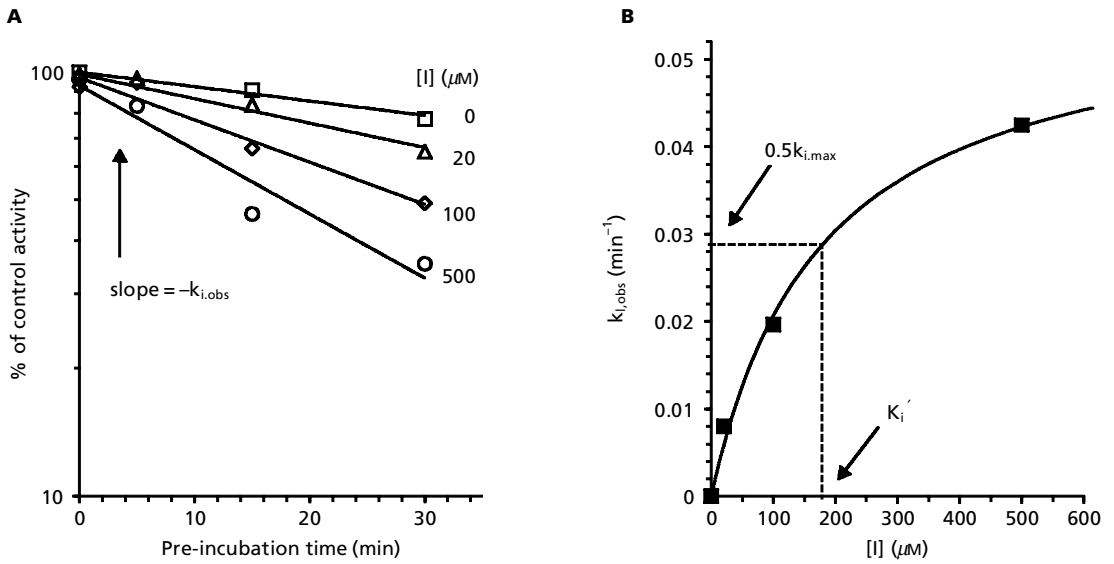

Figure 6 Inhibitory effect of mometasone furoate (MF) 6β-hydroxylation by troleandomycin, shown by (A) the catalysing activity of rat liver microsomes to 6β-hydroxylation of MF in the presence of troleandomycin at various concentrations versus pre-incubation time relative to those of controls, and (B) the values of the apparent inactivation rate constant ($k_{i,obs}$) versus the initial concentrations of troleandomycin. The parameters $k_{i,max}$ and K_i' were estimated using Equation 2 by the least-square method. Incubation of MF ($C_0 = 1.6\,\mu$M) was carried out for 8 min at 37 °C after pre-incubation of troleandomycin (20, 100 and 500 μM) in pooled rat liver microsomes (protein 0.2 mg mL^{-1}) for 0, 5, 15 and 30 min.

When multiple enzymes are involved in the reaction and the low affinity enzymes possess high capacity that is not saturable under the experimental conditions, Equation 6 can be simplified to Equation 7.

$$\nu = \frac{V_{max1} \cdot [MF]}{K_{m1} + [MF]} + CL_i \cdot [MF] \quad (7)$$

where CL_i represents V_{max}/K_m, the intrinsic clearance of a drug due to the enzymes having low affinity but high capacity. Equation 7 has one parameter less than Equation 6, thus estimation of parameters for the high-affinity enzyme(s) can be more reliable. Since in-vivo drug concentrations can rarely exceed the K_m of the low-affinity enzyme(s), the high-affinity process usually accounts

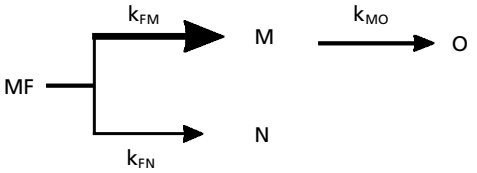

Figure 7 The scheme for the in-vitro biotransformation of mometasone furoate (MF) in rat liver microsomes. k_{FM}, k_{FN}, and k_{MO} are the rate constants of corresponding reactions.

for the majority of net intrinsic clearance. Therefore, characterization of the high-affinity process is generally of most clinical importance.

When the kinetic data set of the parent drug metabolism was tested with Equation 7, a good correlation with the simulated data was obtained (Figure 3; $r^2 = 0.9927$, MSC = 3.6; SCIENTIST). Moreover, the kinetic parameters for the high-affinity catalyst (V_{max1} and K_{m1}) were comparable with those for 6β-hydroxylation (Table 2). The intrinsic clearance of MF via the low-affinity enzymatic reaction was approximately 6.5% of that through the high-affinity metabolic pathway, 6β-hydroxylation.

In addition to the Eadie-Hofstee plots, the biphasic and monophasic Michaelis-Menten models were assessed using plots from transformed kinetic data, for the total loss of MF and the specific loss due to 6β-hydroxylation, respectively. The Lineweaver-Burk plot, illustrating substrate–activity relationships (1/v vs 1/[MF]), became a curvilinear line for MF disappearance, but formed an almost straight line for 6-hydroxy-MF formation. The kinetic parameters (Table 2) for the catalysing enzymes were estimated from the intercepts shown on the graphs. These data suggest the presence of multiple enzymes or multiple isoforms of the enzyme involved in the in-vitro metabolism of MF in rat liver microsomes, in which a single enzyme or enzymes of similar affinity are responsible for its 6β-hydroxylation with the remainder for other reaction(s). Furthermore, the Hanes plot ([MF]/v ratio versus [MF]) for the total loss of MF also displayed biphasic nature, whereas that for the specific loss via 6-hydroxylation was again apparently monophasic in nature. The kinetic parameters for the enzyme systems displaying different roles (Table 2) were estimated from the slopes and intercepts on the plots. From the nature of the plots, it was also evident that the in-vitro metabolism of MF was mediated by multiple enzymes of distinct affinity and capacity, while the 6β-hydroxylation was apparently catalysed by a single enzyme or enzymes of similar affinity.

The values of kinetic parameters estimated for MF 6β-hydroxylation from the three plots were rather close to those generated using the simple Michaelis-Menten equation based on the experimental data (Table 2). For the disappearance of the parent drug, the parameters derived from the lines arbitrated to two-enzyme kinetics were also similar among the three plots. However, there was a discrepancy between the values obtained from these plots and those from the biphasic kinetics (Equation 7), except for V_{max} of the high-affinity process. It is known that monophasic kinetics does not mean that a reaction is

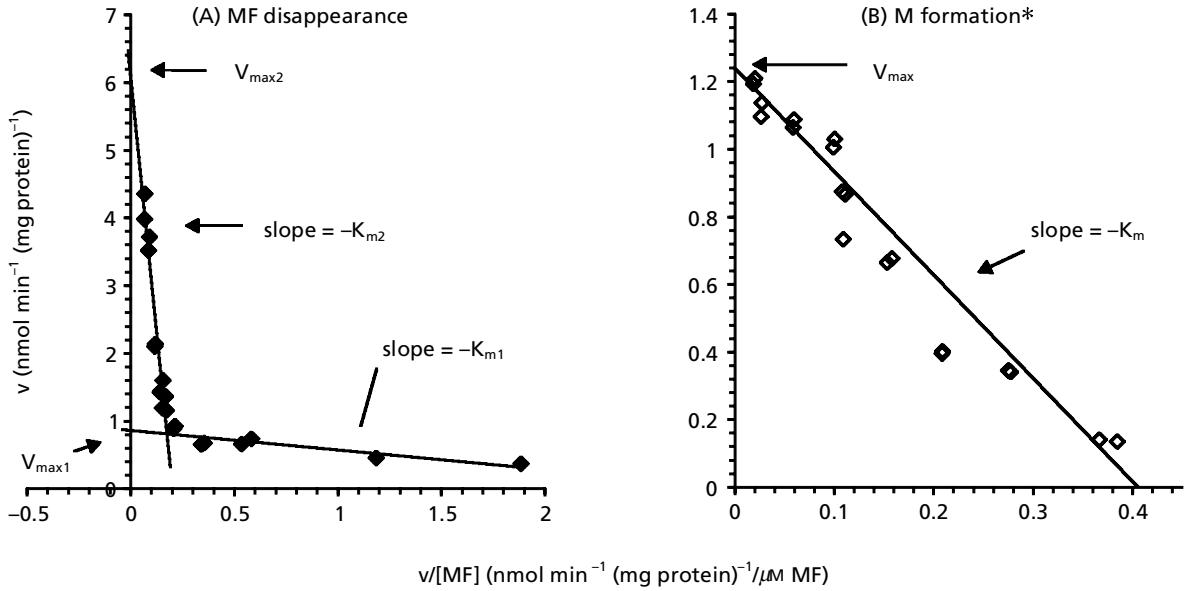

Figure 8 Eadie-Hofstee plots for (A) mometasone furoate (MF) disappearance and (B) 6β-hydroxy-MF (M) formation following the incubation of MF of initial concentration ranging from 0.2 to 65 μM in pooled rat liver microsomes (protein 0.2 mg mL^{-1}) at 37°C. The lines in graph (1) were fitted by $y = -0.288x + 0.8614$ ($r^2 = 0.7905$) and $y = -30.245x + 6.0795$ ($r^2 = 0.9275$), respectively, and the straight line in graph (2) was $y = -2.8436x + 1.1838$ ($r^2 = 0.9279$). *The concentration of M formed is expressed relative to the MF concentration, assuming equal HPLC/UV response.

Table 2 Kinetic parameters for mometasone furoate (MF) disappearance and 6β-hydroxy-MF (M) formation in pooled rat liver microsomes.

Methods/plots	V_{max1} (nmol $min^{-1}mg^{-1}$)	V_{max2} (nmol $min^{-1}mg^{-1}$)	K_{m1} (μM)	K_{m2} (μM)	V_{max1}/K_{m1} (mL $min^{-1}mg^{-1}$)	V_{max2}/K_{m2} (mL $min^{-1}mg^{-1}$)	V_{max}/K_m (mL $min^{-1}mg^{-1}$)
MF disappearance							
Equation 7	1.09		1.32		0.83	0.05	0.88
Eadie-Hofstee	0.86	6.08	0.29	30.25	2.97	0.20	3.17
Lineweaver-Burk	0.81	5.81	0.24	28.41	3.50	0.21	3.71
Hanes	1.00	6.20	0.59	30.53	4.16	0.20	4.36
M formation							
Michaelis-Menten	1.24		2.15		0.58		0.58
Eadie-Hofstee	1.18		2.84		0.42		0.42
Lineweaver-Burk	1.01		2.13		0.47		0.47
Hanes	1.25		2.17		0.58		0.58

M formed is expressed as relative to MF concentration, assuming equal HPLC/UV response.

only mediated by one enzyme. Accordingly, biphasic kinetics implies the involvement of at least two distinct catalysing systems. If the actual number of isoenzymes is greater than two, the Michaelis constant K_m may be a hybrid parameter and, consequently, could probably be intermediate between the actual values of individual isoenzymes.

Discussion

MF is clinically administered as an oral inhaler as well as a nasal aerosol. After administration via the nasal or inhaled routes, only about 20% of the drug enters the lung and the remainder is swallowed and will enter the gastrointestinal tract first and then the liver, and then the lung, before entering the systemic circulation (Barns 1995; Allen 2000). The metabolic and degradation kinetics of MF in these first pass organs were therefore studied. Because of the low solubility of MF (British Pharmacopoeia 2000), after aerosol administration, its initial local concentrations in the lung, the gastrointestinal tract and perhaps the liver on the first pass will likely be significantly higher than systemic concentrations. Thus, the initial concentration of MF in the current study was at the micromolar level.

The overall transformation pattern of MF in rat serum and rat urine was qualitatively similar to that observed in simulated lung fluid (Teng et al 2001). Although a more rapid decomposition of MF occurred in rat serum, relatively smaller amounts of product A but greater amounts of product B were obtained, compared with that in the urine. It has been previously reported that plasma proteins can protect hydrocortisone from autoxidation to 21-dehydrocortisol in buffer of higher pH (Monder 1968). Based on unpublished data, MF is highly (98–99%) bound to human plasma protein (Sharpe and Jarvis 2001). However, the presence of serum proteins did not protect MF from decomposition in the current study. Conversely, a higher apparent degradation of MF with a higher formation of B but not A was observed in rat serum. This might be a result of the catalytic effect of rat serum towards B formation, and/or stabilization of compound B by some component(s) in rat serum.

To identify the site(s) of metabolism for MF in rats, S-9 fractions of different tissues, including liver, intestine, stomach, lung, kidney and spleen, were examined with or without the cofactors. The formation of 6β-hydroxy-MF was found to be catalysed by NADPH-dependent enzymes in the liver in a protein concentration-dependent manner, whereas the formation of products A, B, C and D was not. The large differences in the rate of MF 6β-hydroxylation between S-9 fractions of rat liver and extrahepatic tissues suggest that MF is mainly metabolized in the liver and minimally in the extrahepatic organs tested in rats in-vitro. This is in accordance with the findings of Andersson et al (1982) that the liver tissue S-9 fraction contains both soluble and microsomal enzymes responsible for the biotransformation of glucocorticoids. Furthermore, the threefold inter-individual variability in the rate of MF 6β-hydroxylation reflects that the enzyme activity associated with the in-vitro metabolic process varies significantly between rats. The S-9 fraction of extrahepatic tissues has been previously shown to present limited activity to catalyse 6β-hydroxylation of some other topical glucocorticoids, such as budesonide (Brattsand et al 1982), methylprednisolone, prednisolone and hydrocortisone (Saitoh et al 1998). In addition, hydrolysis of the ester group at C-21 has been found to be much more extensive than that at C-17 (Ronca-Testoni 1983; Andersson & Ryrfeldt 1984). Accordingly, the C-17 steroidal ester MF and its products A, B and C would not be expected to have significant hydrolysis in extrahepatic tissues. This could be the reason why MF was relatively stable in rat extrahepatic tissues. Zbaida et al (1997) reported that MF was not metabolized by lung microsomes from rat, mouse, dog and human. In the present study, the S-9 fraction of rat lung tissue expressed some

ability in catalysing metabolism of MF. The discrepancy may have resulted from differences in experimental conditions and assay methods.

To elucidate the intracellular site of MF metabolism in rat liver, incubations of MF were further performed in nuclear, mitochondrial, cytosolic and microsomal fractions of liver tissue. The results indicated that rat liver microsomes were the primary host of enzymes responsible for MF 6β-hydroxylation. To further investigate the contribution of individual CYP isoenzymes to MF 6β-hydroxylation in rat liver microsomes, a number of potent and/or selective chemical inhibitors and/or substrates used in previous studies were employed. The competitive inhibitory effect by ketoconazole was clearly indicated by the characteristic intersecting points of the fitted lines in the Dixon, Lineweaver-Burk and Eadie-Hofstee plots, as well as the parallel lines in the Cornish-Bowden plots. In the present investigation, the apparent K_i is roughly equivalent to the degree of potency of ketoconazole in the inhibition of testosterone 6β-hydroxylation in rat liver microsomes (IC50 = 0.29 μM; Eagling et al 1998). In addition, the apparent K_i here showed little dependence on the 100-fold ketoconazole concentration as indicated by the low standard deviation. This implied that the inhibitory effect present at low concentrations of ketoconazole was not confounded by its increased concentration. Therefore, the reaction could be mainly catalysed by CYP3A. In addition, the concentration and pre-incubation time-dependent inhibition by troleandomycin (Figure 6A), a selective inhibitor of rat liver CYP3A (Delaforge et al 1988), further suggested the contribution of CYP3A. The concentration-dependent inhibition by diazepam might be owing to its competitive effect on CYP3A, which contributes to diazepam C3-hydroxylase in rat liver (Neville et al 1993). However, the possible involvement of CYP2C11 could not be simply discounted since diazepam is also a substrate of CYP2C11 for diazepam *N*-demethylation in rat liver microsomes (Neville et al 1993). The inhibitory effect by 4-methylpyrazole at very high concentrations implied possible involvement of CYP2E1 (Yamazaki et al 1992) and/or 2D1 (Clarke 1998), the equivalent enzyme in the rat to human CYP2D6 (Umehara et al 1997). The involvement of CYP2D1, however, was not supported by the test with quinidine. The latter is a selective and potent CYP2D1 inhibitor with an effective concentration of 5 μM (Umehara et al 1997), but did not display marked inhibition at concentrations as high as 100 μM. Owing to the low selectivity of diethyldithiocarbamate in rat liver microsomes (Eagling et al 1998), it was not able to distinguish the role of individual CYP isoforms (CYP1A2, 2C, 2E1 and 3A) in this reaction, although it caused marked inhibition of MF 6β-hydroxylation. Among the related CYP families of this inhibitor, CYP1A2 appeared not to be involved because no significant inhibition was obtained with high concentrations of furafylline, an inhibitor of CYP1A2 in rat liver microsomes (Hu & Bunce 1999). In addition, CYP2A appeared not to be responsible for the in-vitro MF 6β-hydroxylation in rat liver since coumarin, a substrate of rat CYP2A3 (Honkakoski & Negishi 1997), did not affect the reaction. The results of the chemical inhibition study suggest that CYP3A can be the major isoenzyme mediating MF 6β-hydroxylation in rat liver, while CYP1A2, 2A3, 2C11, 2D1 were not likely to be involved. The contribution of other CYP isoforms, such as CYP2B, 2E1 and 2C11, was not clearly defined. Further studies are needed to verify these findings and to further clarify the responsibility of individual CYP isoforms through reaction phenotyping using antibodies against individual rat CYP isoforms, purified or cDNA expressed enzymes and through correlation studies using inter-individual variability in expression of the responsible CYP isoforms. Although there are some species differences in the CYP isoform responsible for xenobiotic metabolism (Correia 1995; Eagling et al 1998), the involvement of CYP3A in 6β-hydroxylation of steroids has been observed in both rats and humans (Clarke 1998; Eagling et al 1998; Kenworthy et al 1999; Obach et al 2001). The preliminary results here may throw some light on the subsequent study and identification of human CYP isoforms contributing to MF metabolism.

Whereas limited metabolism of MF was observed in S-9 and microsomal fractions of rat intestinal tissue, considerable metabolism of MF was observed with everted rat intestine. This agrees with the previous finding that MF is metabolized moderately in everted intestines of rat, mouse and dog, with formation of 6β-hydroxy-MF (Zbaida et al 1997). These results are also consistent with the knowledge that everted sacs of mouse small intestine exhibited a high catalytic activity in the metabolism of another steroid, testosterone (Emoto et al 2000). These findings indicate that the small intestine could also be a site of pre-systemic metabolism for MF. Additionally, an important finding is that the rapid disappearance of the MF from the incubation buffer was not solely due to metabolism of MF by the intestinal tissue. In fact, while MF was metabolized by the everted intestine, the parent drug and the metabolite formed were taken up rapidly into the intestinal tissue during the incubation. At the end of the incubation (5 h), the majority of MF (~88%) and 6β-hydroxy-MF (~80%) remained in the intestinal tissue, and small amounts of both the parent drug (~3%) and the metabolite (~4%) were detected in buffer in the sac. Thus, the loss of MF from the incubation buffer was primarily a result of uptake by the intestinal tissue and secondly metabolism. The rapid drug uptake by tissue could be due to binding to tissue proteins, partitioning into the adipose portion of the tissue and membrane lipid bilayer, because of the lipophilic nature of both MF and the metabolite.

In summary, the present in-vitro kinetic studies reveal the qualitative and quantitative differences in the in-vitro biotransformation profiles of MF in different rat tissues. In rat urine and serum, MF degrades to A, B, C and D, following the chemical degradation pathways of MF that also observed in buffer solutions. In-vitro, MF is metabolized rapidly and extensively in rat liver, minimally in rat extrahepatic tissues tested. Under the experimental conditions, 6β-hydroxy-MF is the primary metabolite of MF. Furthermore, in rat liver, microsomes are the major host of enzymes mediating this biotransformation. In particular, CYP3A is the major CYP 450 enzyme respons-

ible for this in-vitro biotransformation of MF in rat liver microsomes. Studies on enzyme kinetics of the in-vitro metabolism of MF indicate that the overall metabolic process in rat liver microsomes follows biphasic Michaelis-Menten kinetics, while 6β-hydroxylation obeys monophasic Michaelis-Menten kinetics. The kinetic parameters derived from the kinetic models along with the enzyme inhibition studies suggest that MF is mainly metabolized by 6β-hydroxylation mediated by CYP3A primarily, and also biotransformed via other pathway(s) catalysed by other enzymes in rat liver in-vitro. In the ex-vivo studies with rat tissues, MF is moderately metabolized in the intestine with 6β-hydroxy-MF as the primary metabolite. In addition, tissue uptake was found to account for the major loss of this drug from the incubation media.

In conclusion, this pre-clinical knowledge may clarify how MF is metabolized in humans given the potential suitability of rat as a model for studying the metabolic kinetics of MF. Furthermore, the ability to optimize and generate metabolite and degradation products of MF has been established. Further studies on MF metabolism kinetics in human and on the pharmacological aspects of the degradation and metabolic products are ongoing.

References

Affrime, M. B., Cuss, F., Padhi, D., Wirth, M., Pai, S., Clement, R. P., Lim, J., Kantesaria, B., Alton, K., Cayen, M. N. (2000a) Bioavailability and metabolism of MF following administration by metered-dose and dry-powder inhalers in healthy human volunteers. *J. Clin. Pharmacol.* **40**: 1227–1236

Affrime, M. B., Kosoglou, T., Thonoor, C. M., Flannery, B. E., Herron, J. M. (2000b) Mometasone furoate has minimal effects on the hypothalamic-pituitary-adrenal axis when delivered at high doses. *Chest* **118**: 1538–1546

Allen, D. B. (2000) Systemic effects of intranasal steroids: an endocrinologist's perspective. *J. Allergy Clin. Immunol.* **106**: S179–S190

Andersson, P., Ryrfeldt, A. (1984) Biotransformation of the topical glucocorticoids budesonide and beclomethasone 17α,21-dipropionate in human liver and lung homogenate. *J. Pharm. Pharmacol.* **36**: 763–765

Andersson, P., Edsbacker, S., Ryrfeldt, A., von Bahr, C. (1982) In vitro biotransformation of glucocorticoids in liver and skin homogenate fraction from man, rat and hairless mouse. *J. Steroid Biochem.* **16**: 787–795

Barnes, P. J. (1995) Drug therapy: inhaled glucocorticoids for asthma. *N. Engl. J. Med.* **332**: 868–875

Brattsand, R., Kallstrom, L., Nilsson, E., Ryrfeldt, A. (1982) The lung disposition of budesonide in guinea pig and rat. *Eur. J. Respir. Dis.* (Suppl.) **122**: 263–265

British Pharmacopoeia (2000) Mometasone furoate. Medicinal and pharmaceutical substances. In: *British Pharmacopoeia* Vol. 1. General Medical Council, Constable & Co., London, pp. 1065–1066

Carcillo, J. A., Korzekwa, K. R., Jones, G. S., Parise, R. A., Gillespie, D. G., Whalen, M. J., Kochanek, P. M., Branch, R. A., Kost, C. K. Jr (1998) The cytochrome P450 suicide inhibitor, 1-aminobenzotriazole, sensitizes rats to zymosan-induced toxicity. *Res. Commun. Mol. Pathol. Pharmacol.* **102**: 57–68

Clarke, S. E. (1998) In vitro assessment of human cytochrome P450. *Xenobiotica* **28**: 1167–1202

Correia, M. A. (1995) Rat and human liver cytochromes P450. In: Ortiz de Montellano, P. R. (ed.) *Cytochrome P450: structure, mechanism and biochemistry*, 2nd edn. Plenum Press, New York, pp. 607–630

Delaforge, M., Sartori, E., Mansuy, D. (1988) In vivo and in vitro effects of a new macrolide antibiotic roxithromycin on rat liver cytochrome P-450: comparison with troleandomycin and erythromycin. *Chem. Biol. Interact.* **68**: 179–188

Doumas, B. T., Bayse, D. D., Carter, R. J., Peters, T. J., Schaffer, R. (1981) A candidate reference method for determination of total protein in serum. I. Development and validation. *Clin. Chem.* **27**: 1642–1650

Eagling, V. A., Tjia, J. F., Back, D. J. (1998) Differential selectivity of cytochrome P450 inhibitors against probe substrates in human and rat liver microsomes. *Br. J. Clin. Pharmacol.* **45**: 107–114

Ekins, S., Mäenpää, J., Wrighton, S. A. (1999) In vitro metabolism: subcellular fractions. In: Woolf, T. F. (ed.) *Handbook of drug metabolism*. Marcel Dekker, New York, pp. 363–399

Emoto, C., Yamazaki, H., Yamasaki, S., Shimada, N., Nakajima, M. T. Y. (2000) Use of everted sacs of mouse small intestine as enzyme sources for the study of drug oxidation activities in vitro. *Xenobiotica* **30**: 971–982

Esposito, G., Csaky, T. Z. (1974) Extracellular space in the epithelium of rats small intestine. *Am. J. Physiol.* **226**: 50–55

Honkakoski, P., Negishi, M. (1997) The structure, function, and regulation of cytochrome P450 2A enzymes. *Drug Metab. Rev.* **29**: 977–996

Hu, K., Bunce, N. J. (1999) Metabolism of polychlorinated dibenzo-*p*-dioxins by rat liver microsomes. *J. Biochem. Mol. Toxicol.* **13**: 307–315

Ito, K., Iwatsubo, T., Kanamitsu, S., Ueda, K., Suzuki, H., Sugiyama, Y. (1998) Prediction of pharmacokinetic alterations caused by drug–drug interactions: metabolic interaction in the liver. *Pharmacol. Rev.* **50**: 387–412

Kenworthy, K. E., Bloomer, J. C., Clarke, S. E., Houston, J. B. (1999) CYP3A4 drug interactions: correlation of 10 in vitro probe substrates. *Br. J. Clin. Pharmacol.* **48**: 716–727

Mathews, J. M., Dostal, L. A., Bend, J. R. (1985) Inactivation of rabbit pulmonary cytochrome P-450 in microsomes and isolated perfused lungs by the suicide substrate 1-aminobenzotriazole. *J. Pharmacol. Exp. Ther.* **235**: 186–190

Monder, C. (1968) Stability of corticosteroids in aqueous solutions. *Endocrinology* **82**: 318–326

Neville, C. F., Ninomiya, S., Shimada, N., Kamataki, T., Imaoka, S., Funae, Y. (1993) Characterization of specific cytochrome P450 enzymes responsible for the metabolism of diazepam in hepatic microsomes of adult male rats. *Biochem. Pharmacol.* **45**: 59–65

Obach, R. S., Zhang, Q.-Y., Dunbar, D., Kaminsky, L. S. (2001) Metabolic characterization of the major human small intestinal cytochrome P450s. *Drug Metab. Dispos.* **29**: 347–352

Ocuma, T., Sato, R. (1964) The carbon monoxide binding pigment of liver microsomes. I. Evidence for its hemoprotein nature. *J. Biol. Chem.* **23**: 2370–2378

Onrust, S. V., Lamb, H. M. (1998) Mometasone furoate. A review of its intranasal use in allergic rhinitis. *Drugs* **56**: 725–745

Pedersen, P. L., Greenawalt, J. W., Reynafarje, B., Hullihen, J., Decker, G. L., Soper, J. W., Bustamente, E. (1978) Preparation and characterization of mitochondria and submitochondrial particles of rat liver and liver-derived tissues. *Methods Cell. Biol.* **20**: 411–481

Pickering, H., Pitcairn, G. R., Hirst, P. H., Bacon, P. R., Newman, S. P., Affrime, M. B., Marino, M. (2000) Regional lung deposition of a technetium 99m-labeled formulation of mometasone furoate administered by hydrofluoroalkane 227 metered-dose inhaler. *Clin. Ther*. **22**: 1483–1493

Prakash, A., Benfield, P. (1998) Topical mometasone. A review of its pharmacological properties and therapeutic use in the treatment of dermatological disorders. *Drugs* **55**: 145–163

Ronca-Testoni, S. (1983) Hydrolysis of cyclomethasone by the human lung. *Int. J. Clin. Pharmacol. Res.* **3**: 17–20

Saitoh, H., Hatakeyama, M., Eguchi, O., Oda, M., Takada, M. (1998) Involvement of intestinal P-glycoprotein in the restricted absorption of methylprednisolone from rat small intestine. *J. Pharm. Sci*. **87**: 73–75

Sharpe, M., and Jarvis, B. (2001) Inhaled mometasone furoate: a review of its use in adults and adolescents with persistent asthma. *Drugs* **61**: 1325–1350

Teng, X. W. (2002) Metabolism and degradation of mometasone furoate. PhD Thesis, University of Sydney

Teng, X. W., Foe, K., Brown, K. F., Cutler, D. J., Davies, N. M. (2001) High-performance liquid chromatographic analysis of mometasone furoate and its decomposition products: application to in vitro degradation studies. *J. Pharm. Biomed. Anal*. **26**: 313–331

Umehara, K., Kudo, S., Odomi, M. (1997) Involvement of CYP2D1 in the metabolism of carteolol by male rat liver microsomes. *Xenobiotica* **27**: 1121–1129

Wang, C. J., Tian, Z., Byrnes, K., Lin, C. C. (1992) A competitive enzyme immunoassay for the direct determination of mometasone furoate (SCH 32088) in human plasma. *J. Pharm. Biomed. Anal*. **10**: 473–479

Yamazaki, H., Oda, Y., Funae, Y., Imaoka, S., Inui, Y., Guengerich, F. P., Shimada, T. (1992) Participation of rat liver cytochrome P450 2E1 in the activation of N-nitro sodimethylamine and N-nitrosodiethylamine to products genotoxic in an acetyltransferase-overexpressing *Salmonella typhimurium* strain (NM2009). *Carcinogenesis* **13**: 979–985

Zbaida, S., Shannon, D., Du, Y., Lu, X., Ng, K., Chowdhury, S., Blumenkrantz, N., Patrick, J., Cayen, M. N. (1997) In vitro metabolism of mometasone furoate (Abstract no. P339). *FASEB* **11** (8 Suppl. S): A829